MAR 3 1982

NAS 1.26:3506

NASA Contractor Report 3506

Ultrasonic Input-Output for Transmitting and Receiving Longitudinal Transducers Coupled to Same Face of Isotropic Elastic Plate

COMPLETED
37

James H. Williams, Jr., Hira Karagulle,
and Samson S. Lee

GRANT NSG-3210
FEBRUARY 1982

NASA

NASA Contractor Report 3506

Ultrasonic Input-Output for Transmitting and Receiving Longitudinal Transducers Coupled to Same Face of Isotropic Elastic Plate

James H. Williams, Jr., Hira Karagulle, and Samson S. Lee
Massachusetts Institute of Technology
Cambridge, Massachusetts

Prepared for
Lewis Research Center
under Grant NSG-3210

National Aeronautics
and Space Administration

Scientific and Technical Information Branch

1982

I

INTRODUCTION

The parameters which govern the mechanical behavior of materials also affect their stress wave propagation characteristics. In particular, stress waves are the interrogating energy in ultrasonic testing (UT) and acoustic emission (AE).

A major technique in UT is "through-transmission" ultrasonics. A mechanical disturbance is introduced into the material by a transducer coupled to one face of the structure and the resulting signal produced by a second transducer which is coupled to the directly opposite face of the structure is analyzed. Wave velocities, material attenuations, and structural thickness can be measured using this technique [1]. Also, cracks can be detected in this manner [2]. And, it has been shown that the inital through transmission longitudinal attenuation can be correlated with the compression fatigue life [3] and the flexural fatigue life [4] of graphite fiber composites.

Another technique is "pulse echo" ultrasonics. Here the transmitting and receiving transducers are mounted on the same face of the structure. The output signal is due to reflections from the other face or a discontinuity inside the material. The transmitting and receiving sensors may be separate or the same transducer.

An ultrasonic parameter in which the transmitting and receiving transducers are coupled to the same face of the structure is called the "Stress Wave Factor" by Vary et al. [5,6]. An input pulse having a broadband frequency spectrum is applied to the transmitting transducer and the number of output oscillations exceeding a certain threshold amplitude is defined as the stress wave factor (SWF). The SWF has been correlated with mechanical properties of graphite fiber epoxy composites [5-7]. For example, Williams, and Lampert [7] showed that as the residual strength of the composite decreases due to impact damage, the stress wave factor decreases and the attenuation measured with the through transmission technique increases. Thus, a correlation between the SWF and attenuation was indicated also.

In this study the output signal due to a single tone burst input will be analyzed theoretically and experimentally for the case where transmitting and receiving transducers are both coupled to the same face of the structure.

If an ultrasonic disturbance is introduced into or is generated within an elastic isotropic structure, the parameters which govern its subsequent propagation and detection may be summarized as follows:

1. Material Properties: Modulus of elasticity, Poisson's ratio, density, shear and longitudinal attenuations, velocity, microstructural defect state,...;

2. Geometrical properties: Overall geometry, discontinuities, macrostructural defect state,...;

3. Measurement conditions: Location and size of transducers, sensitivity and frequency response of transducers, couplant, frequency and amplitude characteristics of input,...

A more extensive list of parameters, including those which must be considered for fiber reinforced composite structures is given by Williams [8]. Various authors have discussed the effects of material anisotropy and macrostructural defect state [9-11] as well as experimental measurement conditions including type and thickness of couplant [12-14] and transducer-structure contact pressure requirements [1].

Finally, while it is clear that the proposed analysis has significant value in ultrasonic testing, it is important to reemphasize that such an analysis is equally valuable in acoustic emission. For example, since both longitudinal and shear waves may be generated by AE events and since both types of waves must propagate through the structure before being detected, it is clear that material properties, geometrical properties and measurement conditions all play a role in what is ultimately detected as the AE signal. Further, since the reflection at boundaries of one type of wave produces the other type, this indicates various coupling effects between the material, geometric and measurement features on both ultrasonic and acoustic emission parameters.

THEORETICAL ANALYSIS

A schematic of the system under investigation is shown in Fig. 1. A transmitting and a receiving transducer of radius a and spaced a distance ℓ apart are coupled to the same face of an isotropic elastic plate of thickness h and of infinite planar (x - y) extent. The input electrical voltage to the transmitting transducer is $V_i(t)$ and the output electrical voltage from the receiving transducer is $V_o(t)$ where t represents time. The output voltage $V_o(t)$ due to a steady-state sinusoidal input voltage $V_i(t)$ are analyzed.

Assumptions on the Transducers

The longitudinal transducers are assumed to transform an electrical voltage into a uniform normal stress and vice versa. The approach which follows is similar to [15].

If an input voltage of amplitude V and frequency ω is applied according to

$$V_i(t) = V e^{-i\omega t} \quad , \tag{1}$$

the normal stress σ_{zz} that is introduced into the specimen at the transducer-specimen interface by the transmitting transducer is

$$\sigma_{zz}(t) = F_1(\omega) V e^{-i(\omega t + \phi_1)} \tag{2}$$

where $F_1(\omega)$ is the transduction ratio for the transmitting transducer in transforming a voltage to a stress and ϕ_1 is a phase angle. In eqns. (1) and (2), the harmonic character of the signals are expressed in the complex notation where $i \equiv \sqrt{-1}$ and only the real parts of these and subsequent equations should be considered. Thus, the amplitude T of the applied stress is defined as

$$T = F_1(\omega) V \tag{3}$$

Similarly, if a stress wave producing a normal stress component σ'_{zz} of amplitude T' and frequency ω that impinges on the receiving transducer is defined as

$$\sigma'_{zz}(t) = T' e^{-i\omega t} , \tag{4}$$

the output voltage from the receiving transducer is

$$V_o(t) = F_2(\omega)\, T' e^{-i(\omega t + \phi_2)} \tag{5}$$

where $F_2(\omega)$ is the transduction ratio for the receiving transducer in transforming a normal stress to a voltage and ϕ_2 is a phase angle. Thus, the amplitude V' of the output electrical voltage is

$$V' = F_2(\omega)\, T' \tag{6}$$

Stress Field Radiated by the Transmitting Transducer

The stress field radiated into an isotropic elastic semi-infinite solid by the transmitting transducer is now considered. Internal reflections from the faces of the plate are considered in a subsequent subsection.

Fig. 2 shows an isotropic elastic half space bounded by the (x - y) plane and extending into the positive z-direction. The semi-infinite medium is excited by a uniform harmonic normal stress over a circular region of radius a at its surface.

Using the cylindrical coordinates (r,ϕ,z) as shown in Fig. 2, the boundary conditions at z = 0 require that the shear stresses σ_{zr} and $\sigma_{z\phi}$ vanish and that the only nonzero stress is the normal stress

$$\sigma_{zz} = \begin{cases} T e^{-i\omega t} & \text{for } 0 \leq r \leq a \\ 0 & \text{for } r > a \end{cases} \tag{7}$$

This is an extension of the so-called Lamb problem [16] and using Hankel transform techniques, Miller and Pursey [17] have derived the displacement field solution at any point in the medium. From the displacements, the normal stress σ_{zz} at any point in the half space can be shown to be

$$\sigma_{zz} = aTe^{-i\omega t}\left[\int_o^\infty \frac{J_1(\xi a)(k_2^2 - 2\xi^2)^2}{G(\xi)} J_o(\xi r)\, e^{i\sqrt{k_1^2 - \xi^2}\, z}\, d\xi \right. \tag{8}$$

$$\left. - 4\int_o^\infty \frac{J_1(\xi a)\sqrt{k_1^2 - \xi^2}\sqrt{k_2^2 - \xi^2}(2k_2^2 - \xi^2)}{G(\xi)} J_o(\xi r)\, e^{i\sqrt{k_2^2 - \xi^2}\, z}\, d\xi \right]$$

where

$$G(\xi) = (2\xi^2 - k_2^2)^2 + 4\xi^2\sqrt{k_1^2 - \xi^2}\sqrt{k_2^2 - \xi^2}$$

$$k_1 = \frac{\omega}{c_1} \tag{9}$$

$$k_2 = \frac{\omega}{c_2}$$

where c_1 is the longitudinal wave speed, c_2 is the shear wave speed, ξ is an integration variable introduced in the Hankel transform, J_o and J_1 are Bessel functions of the first kind and of order zero and one, respectively.

The asymptotic behavior of eqn. (8) for large R and small a can be obtained using procedures in [17] as

$$\sigma_{zz} \simeq iaT\left[D_1(\omega,\theta)\frac{e^{ik_1(R - c_1 t)}}{R} - 4D_2(\omega,\theta)\frac{e^{ik_2(R - c_2 t)}}{R}\right] \tag{10}$$

where

$$D_1 = \frac{\cos\theta\,(k^2 - 2\sin^2\theta)^2 J_1(k_1 a \sin\theta)}{\sin\theta\,[(k^2 - 2\sin^2\theta)^2 + 4\sin^2\theta\cos\theta\sqrt{k^2 - \sin^2\theta}\,]}$$

$$D_2 = \frac{\cos\theta\,(2 - \sin^2\theta)\sqrt{1 - k^2\sin^2\theta}\; J_1(k_2 a \sin\theta)}{\sin\theta\,[k(2\sin^2\theta - 1)^2 + 4\sin^2\theta\cos\theta\sqrt{1 - k^2\sin^2\theta}\,]} \tag{11}$$

and

$$k = \frac{c_1}{c_2} = \frac{k_2}{k_1}$$

The first term in the square bracket in eqn. (10) propagates with the longitudinal (P) wave velocity c_1. Thus, this normal stress component is associated with the so-called P-wave. The second term is the square bracket in eqn. (10) propagates with the shear (S) wave velocity c_2. Thus, this normal stress component is associated with the so-called S-wave. The factors D_1 and D_2 are functions of frequency ω and angle θ and are the directivity functions for the P and S waves, respectively. Fig. 3 shows polar diagrams of the directivity function D_1 associated with the P-wave for various frequencies.

Near Field and Far Field

The asymptotic solution given by eqn. (10) is valid for large R or the far field. In order to determine the magnitude of R at which the asymptotic solution becomes valid, the truncated terms in the asymptotic evaluation of eqn. (8) should be investigated. However, by using an analogy with a similar acoustics problem, an estimate for the far-field distance can be obtained readily.

The acoustics problem considered is a rigid piston vibrating in a rigid baffle. The radiation pressure along the piston axis in the acoustic medium is of interest and is given in [18]. The amplitude of the radiation pressure fluctuates near the piston and eventually approaches the asymptotic solution given in [19]. The near-field distance z_o within which rapid pressure fluctuations occur is [20]

$$z_o = \frac{4a^2 - \lambda^2}{4\lambda} \tag{12}$$

where λ is the wavelength. Then the far field distance z_F where the asymptotic solution applies is given as [2]

$$z_F \simeq 3z_o \tag{13}$$

Combining eqns. (12) and (13), the P-wave component of σ_{zz} given in eqn. (10) is valid if

$$R > R_{F_1} = 3\,\frac{4a^2 - \lambda_1^2}{4\lambda_1} \tag{14}$$

where R_{F_1} is the far-field distance and λ_1 is the longitudinal wavelength and is given by

$$\lambda_1 = \frac{2\pi c_1}{\omega} \tag{15}$$

Wave Reflection at a Plane Boundary

Waves in the plate specimen experience multiple reflections between the faces of the plate. An obliquely incident plane P-wave is reflected from the boundary as a P-wave with an angle of reflection equal to the angle of incidence, say θ_1, and with a S-wave with an angle of reflection, say θ_2, where θ_1 and θ_2 are related by Snell's law as [9]

$$\sin \theta_1 = \frac{c_1}{c_2} \sin \theta_2 \tag{16}$$

The magnitudes of the reflected P and S waves are defined by the reflection coefficients Q_{PP} and Q_{PS}, respectively, and are given by [9]

$$Q_{PP} = \frac{\sin 2\theta_1 \sin 2\theta_2 - k^2 \cos^2 2\theta_2}{\sin 2\theta_1 \sin 2\theta_2 + k^2 \cos^2 2\theta_2} \tag{17}$$

and

$$Q_{PS} = \frac{2 \sin 2\theta_1 \cos 2\theta_2}{\sin 2\theta_1 \sin 2\theta_2 + k^2 \cos^2 2\theta_2} \tag{18}$$

Spherical waves are generated in the plate specimen shown in Fig. 1. However, incident and reflected spherical waves are nearly plane near the boundary of reflection if the wavelengths are much smaller than the distance travelled by the wave from the wave source to the boundary [21]. Then, the plane wave reflection solution given in eqns. (16) through (18) applies.

Steady-State Output Voltage Amplitude due to Multiple Wave Reflections in a Plate

Fig. 4 illustrates a plate of thickness h with a transmitting transducer located at point 0 and a receiving transducer located on the same face at point M, separated by a distance ℓ. A path in the plate is also shown where the wave is reflected n times from the bottom face of the plate. Only P-waves are considered in what follows. The total number of reflections experienced by the wave in travelling from the transmitting transducer to the receiving transducer is (2n - 1). With respect to z the angle of incidence of the wave at either face of the plate is θ_1 and the total distance travelled by the wave is R_n. From the geometry in Fig. 4,

$$\theta_1 = \tan^{-1} \left(\frac{\ell}{2nh}\right) \tag{19}$$

and

$$R_n = \frac{\ell}{\sin \theta_1} \tag{20}$$

The time delay t_n for the wave to reach the receiver after n reflections from the bottom face is

$$t_n = \frac{R_n}{c_1} \tag{21}$$

If there were no bottom boundary and the waves were propagating in an infinite half space, the waves would travel to point M' in time t_n. Then the amplitude of the hypothetical normal stress at point M' is $T_{M'}$ and is defined per eqn. (10) as

$$T_{M'} = \frac{aT D_1}{R_n} \tag{22}$$

However, with the bottom boundary present, the wave is reflected a total of (2n - 1) times. Thus the amplitude of the normal stress at point M is T_M and is obtained by modifying eqn. (22) as

$$T_M = \frac{aT D_1 Q_{PP}^{2n-1}}{R_n} \tag{23}$$

where Q_{pp} is given in eqn. (17). The amplitude of the output voltage from the receiving transducer is V_n and can be obtained by combining eqns. (6) and (23) as

$$V_n = \frac{F_2 a T D_1 Q_{pp}^{2n-1}}{R_n} \tag{24}$$

Substituting eqn. (3) into eqn. (24) gives

$$V_n = \frac{F_1 F_2 V a D_1 Q_{PP}^{2n-1}}{R_n} \tag{25}$$

Introducing the longitudinal wave attenuation constant α of the medium and a possible signal amplification factor K, eqn. (25) can be rewritten as

$$V_n = K F_1 F_2 V a D_1 Q_{PP}^{2n-1} \frac{e^{-\alpha R_n}}{R_n} . \tag{26}$$

Eqn. (26) gives the output voltage amplitude from the receiving transducer due to an input voltage amplitude V at the transmitting transducer when the wave path has included n reflections from the bottom face of the plate specimen. Only P-waves have been considered and eqn. (26) is valid if the plate thickness h is larger than the far-field distance R_{F_1}.

EXPERIMENTAL EQUIPMENT AND PROCEDURES

A schematic of the experimental system is shown in Fig. 5. The system consisted of a pulsed oscillator (Arenburg model PG-652C) for generating the sinusoidal waves; a low frequency inductor (Arenburg model LFT-500); a low frequency amplifier (Arenburg model LFA-550); broadband (0.1 to 3.0 MHz) transmitting and receiving transducers (Acoustic Emission Technology (AET) FC-500) having an approximately flat sensitivity of -85 dB (relative to 1V/μBar); a transducer specimen interface couplant (AET SC-6); and an oscilloscope (Tektronix model 455). An attenuator, set at 10 dB, reduced the input signal to 100 V (peak-to-peak) into the transmitting transducer.

The specimen was an aluminum (6061-T6) plate 10 cm in thickness and 25 cm on a side. The plate specimen was supported by a 2.5 cm wide rubber mount on the bottom face. The diameter of the wearplate of the FC-500 transducer was 2.25 cm and the clamping pressure on the transducer exceeded the saturation pressure which is defined in [1] as the minimum transducer-specimen interface pressure which results in the maximum amplitude of the output signal, all other parameters being held constant.

A single 100 V peak-to-peak tone burst (finite duration sinusoidal signal) was input into the transmitting transducer. The output from the receiving transducer was recorded at various spacings between the transducers and tone burst input frequencies. The duration of the tone burst input was chosen so that the output signals due to multiple reflections did not overlap. The input frequencies were 0.75, 1.50 and 2.25 MHz. The transducer spacings (ℓ) between the transducer axes were 5.5 and 10.0 cm.

The aluminum had a density of 2.7 g/cm^3; longitudinal wave velocity of 6.32 x 10^5 cm/sec [2]; shear wave velocity of 3.13 x 10^5 cm/sec [2]; surface or Rayleigh wave velocity of 2.93 x 10^5 cm/sec [9]; and longitudinal wave attenuation of 0.015 neper/cm [22]. Note that it was assumed that the longitudinal wave attenuation was constant for the frequencies considered.

RESULTS AND DISCUSSIONS

Typical input and output signal records are shown in Fig. 6. The input signal frequency was 1.50 MHz and the transducer separation was 5.5 cm. The time delays for multiple reflections are indicated both above and below the output record. The notations P, S and R represent the longitudinal, shear and Rayleigh waves, respectively. Also the notations P-P and P-S represent a P-wave reflected from the bottom face producing a P and a S wave, respectively.

Fig. 6 shows that the output signal is dominated by reflections of P-waves only. (Refer to the time delays above the output record.) Because the specimen is finite in its planar dimensions, reflections from the vertical faces began to appear after the 6th reflection from the bottom face. Fig. 6 also shows that for this special case, the 2nd reflection from the bottom face produces the output wave packet having the maximum amplitude.

Table 1 shows the calculated and measured time delays t_n for the P-waves to reach the receiving transducer after multiple reflections from the bottom face. The calculated values are based on eqn. (21). The measured values are accurate to within 1 μs. Table 1 shows that there is excellent agreement between the calculated and measured time delay values.

Theoretical results based on eqn. (26) are plotted with the experimental results in Figs. 7 through 10. The vertical axis represents the amplitude of the output signal of each reflection from the bottom face. The horizontal axis is the time scale indicating the time delay for each reflection to travel from the transmitting transducer to the receiving transducer. Only P-waves are considered. Because the factor F_1F_2 in eqn. (26) is not known, the theoretical result is arbitrarily specified to match the experimental result at the 4th reflection. (In fact, this may be considered a technique for estimating F_1F_2.) Fig. 7 is obtained at 0.75 MHz with a transducer spacing of 5.5 cm; Fig. 8 is obtained at 1.50 MHz with a transducer spacing of 5.5 cm; Fig. 9 is obtained at 1.50 MHz with a transducer spacing of 10.0 cm and Fig. 10 is obtained at 2.25 MHz with a transducer spacing of 5.5 cm.

There is good agreement between the theoretical and experimental data in Figs. 7 to 10. In every case, the maximum discrepancy between the theoretical and experimental data occurs for the first reflection from the bottom face. The probable reasons for this discrepancy are one or more of the following:

1. The theoretical analysis assumes that the receiving transducer produces an output voltage that is proportional to the normal stress applied to its face. However, only the normal stress at the center of the receiving transducer is used in the study. The normal stress varies over the transducer face depending on the angle of incidence, the

wavelength and the transducer diameter. Given the same wavelength and the same transducer diameter within a test, the maximum error will occur when the angle of incidence is largest; and this happens for the first reflection.

2. The theoretical study considers a steady-state input with a single frequency. However, the tone burst input used in the experiments has a finite duration. Thus, the input frequency spectrum has a finite bandwidth. Yet, only the center frequency of the spectrum is considered in the theoretical calculations. From Fig. 3, it is observed that at large angles of incidence, the directivity function gives decreasing values of amplitude for increasing frequencies. Thus for the first reflection where the angle of incidence is largest, the error is expected to be largest compared with other reflected waves because the higher frequency content of the spectrum has been drastically reduced by the directivity function. This results in the greater distortion of the signal recorded by the receiver for the first reflection as shown in Fig. 6. Furthermore, these arguments suggest that the theoretical prediction of the amplitude of the first reflected wave should exceed the experimentally measured amplitude. This is consistent with Figs. 7 through 10.

3. The theoretical solution in eqn. (26) is based on an asymptotic approximation for distances larger than the far-field distance R_{F_1}. The far-field distance for 0.75, 1.50 and 2.25 MHz are calculated using eqn. (14) to be 3.89, 8.73 and 13.35 cm, respectively. The thickness of the plate specimen is 10.0 cm. Because the distance travelled by the first reflected wave is less compared to other reflected waves, the error in the asymptotic theoretical solution is expected to be larger for this first reflected wave.

CONCLUSIONS

Ultrasonic input-output characteristics for an isotropic elastic plate with transmitting and receiving longitudinal transducers coupled to the same face have been analyzed theoretically and experimentally.

In the theoretical analysis, it was assumed that the transmitting transducer applied a uniform normal stress to the specimen surface when the transducer was excited by an electrical voltage. The normal stress field in the plate was calculated via a boundary value problem for an isotropic elastic semi-infinite medium subjected to a uniform normal stress applied to a circular region at the surface and varying harmonically in time. An asymptotic solution for the normal stress field was obtained and the frequency and geometric dependent directivity functions for the radiated stress field were found. The requirement for the asymptotic solution to be valid was also discussed. Then, the radiated stress waves were confined to the plate specimen by considering wave reflections at the top and bottom faces. Reflection coefficients were used to describe the wave reflections behavior at the faces. By introducing material attenuation and by assuming that the receiving transducer transforms the incident normal stress into an electrical voltage, the output voltage amplitude of the receiver was derived. Particular attenuation was given to the P-waves only.

There was good agreement between the theoretical and experimental results for the output voltage amplitudes due to multiple reflections of longitudinal waves. Similarly, excellent agreement between the theoretical and experimental results for the times-of-arrival of the individual wave packets at the receiving transducer were obtained.

This study provides a major step forward in the quantitative understanding of ultrasonic nondestructive evaluation (NDE) parameters such as the stress wave factor (SWF). It also provides the potential for assisting in the development of more efficient and more revealing NDE schemes utilizing the SWF. Acoustic emission, ultrasonic attenuation measurements as well as transducer calibration techniques may also benefit from this study. Finally, this work should be extended to the interrogation of composite materials.

REFERENCES

1. J.H. Williams, Jr., H. Nayeb-Hashemi and S.S. Lee, "Ultrasonic Attenuation and Velocity in AS/3501-6 Graphite Fiber Composite", Journal of Nondestructive Evaluation, Vol. 1, No. 2, 1980, pp. 137-148.

2. J. Krautkramer and H. Krautkramer, "Ultrasonic Testing of Materials", Second Edition, Springer-Verlag, NY, 1977.

3. J.H. Williams, Jr. and B. Doll, "Ultrasonic Attenuation as an Indicator of Fatigue Life of Graphite Fiber Epoxy Composites", Materials Evaluation, Vol. 38, No. 5, May 1980, pp. 33-37.

4. J.H. Williams, Jr., H. Yuce and S.S. Lee, "Ultrasonic and Mechanical Characterizations of Fatigue States of Graphite Epoxy Composite Laminates", Composite Materials and Nondestructive Evaluation Laboratory, Massachusetts Institute of Technology, Cambridge, Massachusetts, October 1981.

5. A. Vary and R.F. Lark, "Correlation of Fiber Composite Tensile Strength with the Ultrasonic Stress Wave Factor", Journal of Testing and Evaluation, Vol. 7, No. 4, 1979, pp. 185-191.

6. A. Vary and K.J. Bowles, "An Ultrasonic-Acoustic Technique for Nondestructive Evaluation of Fiber Composite Quality", Polymer Engineering and Science, Vol. 19, No. 5, April 1979, pp. 373-376.

7. J.H. Williams, Jr. and N.R. Lampert, "Ultrasonic Evaluation of Impact-Damaged Graphite Fiber Composite", Materials Evaluation, Vol. 38, No. 12, December 1980, pp. 68-72.

8. J.H. Williams, Jr., "Wave Propagation in Fiber Composites Relating to Acoustic-Ultrasonic NDE Techniques", A Proposal submitted to the NASA Lewis Research Center, July 1981.

9. K.F. Graff, "Wave Motion in Elastic Solids", Ohio State University Press, Ohio, 1975.

10. J.D. Achenbach, "Wave Propagation in Elastic Solids", North-Holland Publishing Company, NY, 1973.

11. J.D. Achenbach, K. Wiswanathan and A. Norris, "An Inversion Integral for Crack Scattering Data", Wave Motion, Vol. 1, No. 4, October 1979, pp. 299-316.

REFERENCES (CONT'D)

12. N.N. Hsu, S.C. Hardy, "Experiments in Acoustic Emission Waveform Analysis for Characterization of AE Sources, Sensors and Structures", Elastic Waves and Nondestructive Testing of Materials, AMD-Vol. 78, Edited by Y.H. Pao, American Society of Mechanical Engineers, 1978, pp. 85-106.

13. R.Hill and S.M.A. El-Dardiry, "A Theory for Optimization in the Use of Acoustic Emission Transducers", Journal of Acoustical Society of America, Vol. 67, No. 2, February 1980, pp. 673-682.

14. A. Vary, "Simulation of Transducer-Couplant Effects on Broadband Ultrasonic Signals", NASA Technical Memorandum 81489, 1980.

15. S.S. Lee and J.H. Williams, Jr., "Stress Wave Attenuation in Thin Structures by Ultrasonic Through-Transmission", (To appear in the Journal of Nondestructive Evaluation.)

16. H. Lamb, "On the Propagation of Tremors Over the Surface of an Elastic Solid", Philosophical Transactions of the Royal Society of London, Series A, Vol. 203, September 1904, pp. 1-42.

17. G.F. Miller and H. Pursey, "The Field and Radiation Impedance of Mechanical Radiators on the Free Surface of a Semi-infinite Isotropic Solid", Proceedings of the Royal Society of London, Series A, Vol. 223, May 1954, pp. 521-541.

18. R.B. Lindsay, "Mechanical Radiation", McGraw Hill, NY, 1960, pp. 251-261.

19. P.M. Morse, "Vibration and Sound", Second Edition, McGraw Hill, NY, 1948, pp. 326-328.

20. G.L. Gooberman, "Ultrasonics-Theory and Application", Hart Publishing Company, NY, 1968, pp. 27-37.

21. L.M. Brekhovskikh, "Waves in Layered Media", Translated by D. Liberman and Edited by R.T. Beyer, Academic Press, NY, 1960.

22. R. Truell and A. Hikata, "Fatigue and Ultrasonic Attenuation", Symposium on Nondestructive Testing, ASTM STP 213, American Society for Testing Materials, 1957, pp. 63-69.

TABLE 1 Calculated and Measured Time Delays for Longitudinal Waves to Reach the Receiving Transducer after Multiple Reflections

Number of Reflections from Bottom Face n	Time Delay t_n, (μs)			
	for ℓ = 5.5 cm		for ℓ = 10.0 cm	
	Calculated	Measured	Calculated	Measured
1	32.8	32	35.4	35
2	63.9	63	65.2	65
3	95.3	95	96.3	96
4	126.9	126	127.6	127
5	158.5	157	159.0	158
6	190.1	188	190.5	188

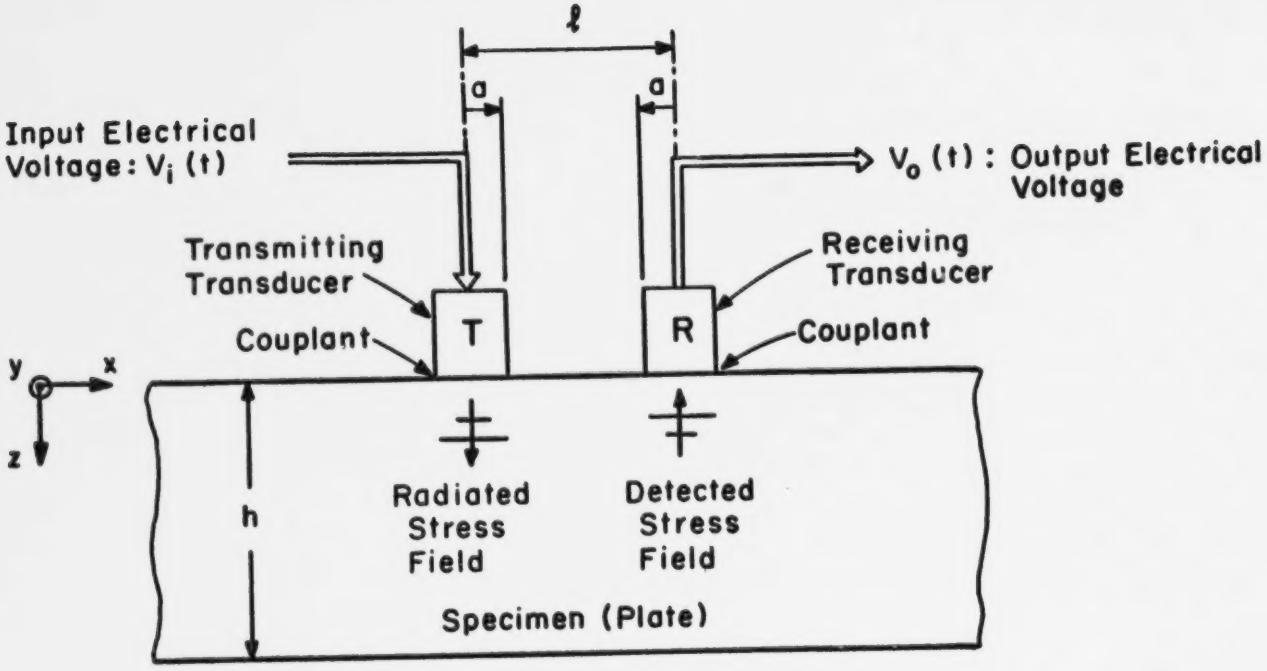

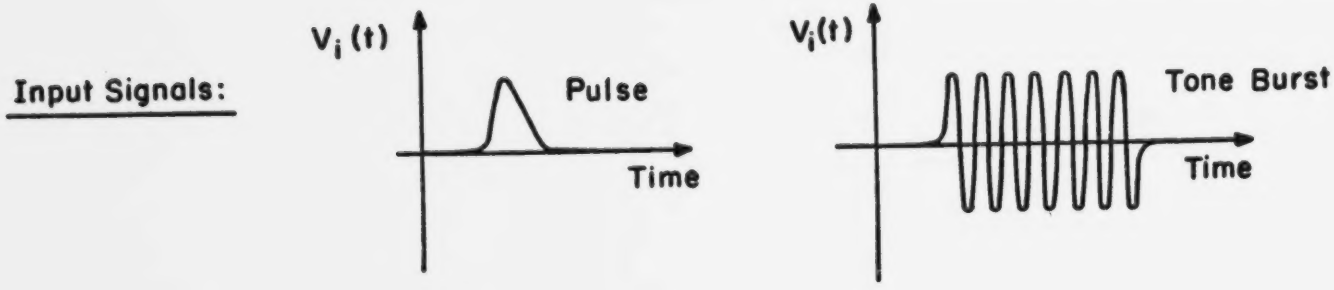

Fig. 1 Schematic of ultrasonic (stress wave factor) configuration showing typical input signals.

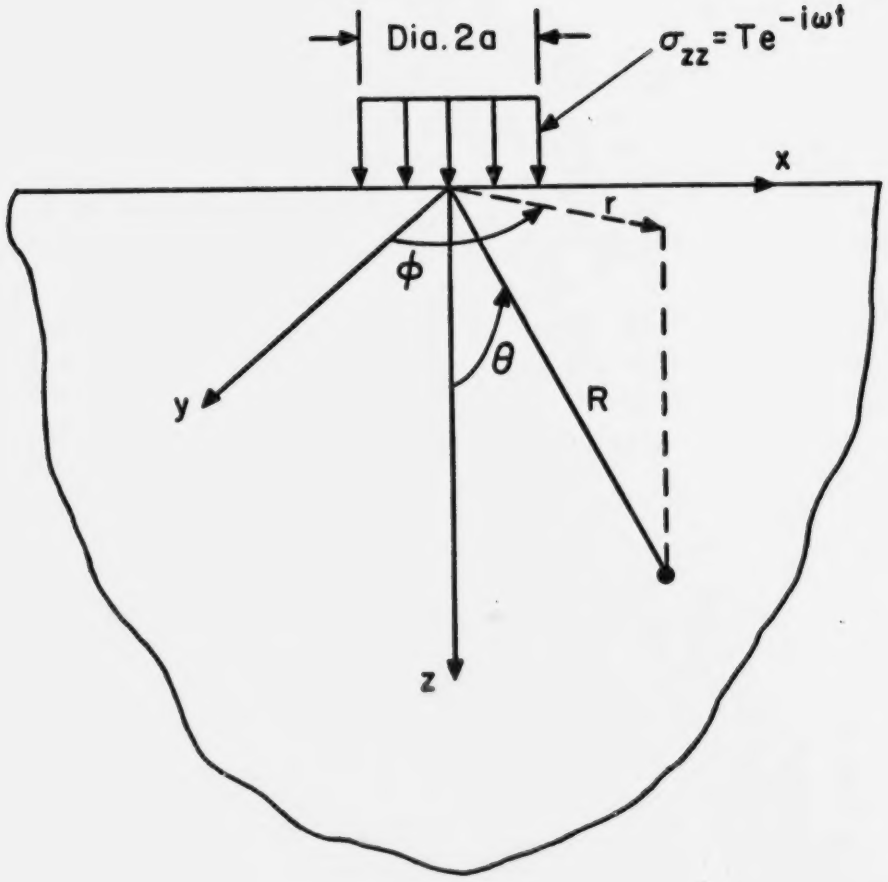

Fig. 2 Half-space problem in evaluating the radiated stress field due to the transmitting transducer in the cylindrical coordinate system (r,ϕ,z).

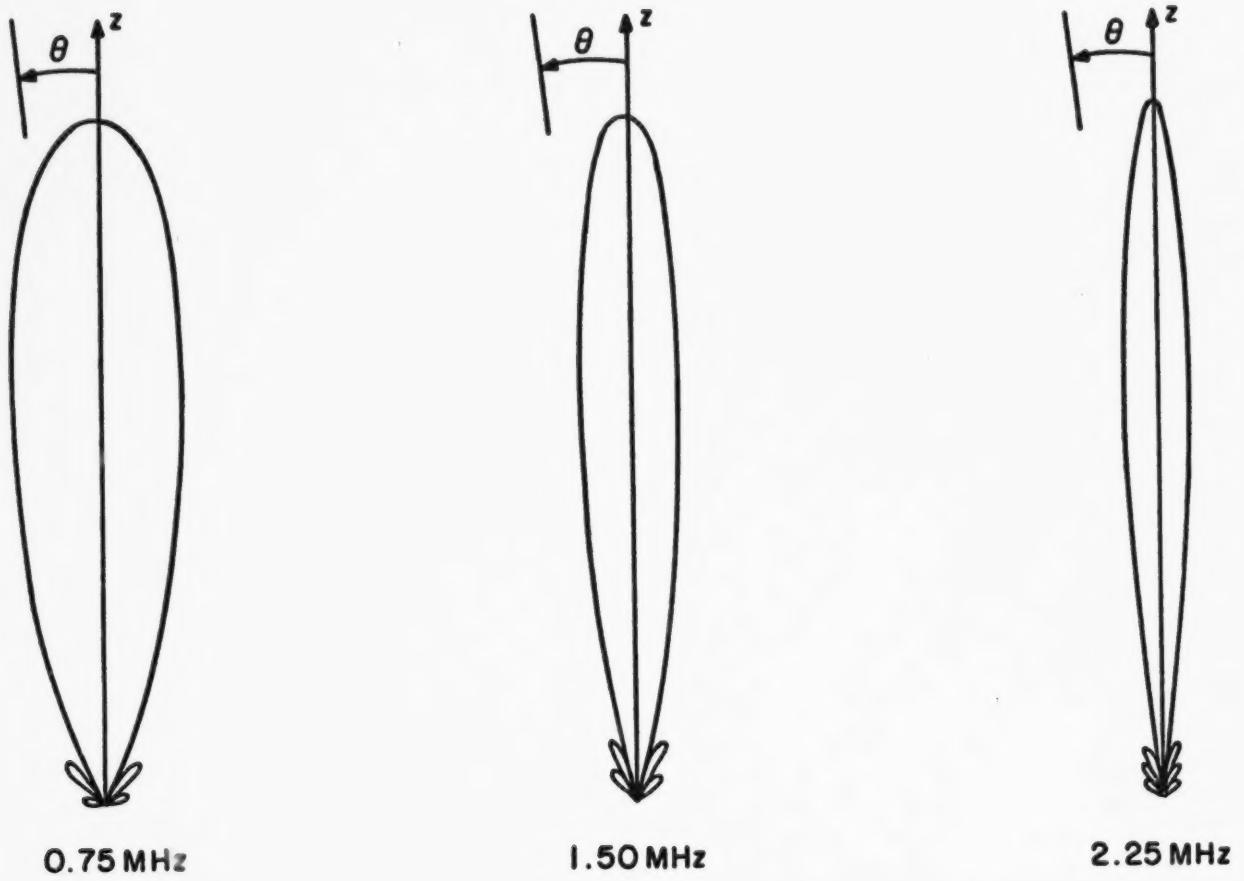

Fig. 3 Polar diagrams of frequency and angle dependent directivity function D_1 for the normal stress due to longitudinal waves with transducer radius a of 1.125 cm, longitudinal wave speed c_1 of 6.32×10^5 cm/sec, and shear wave speed c_2 of 3.13×10^5 cm/sec.

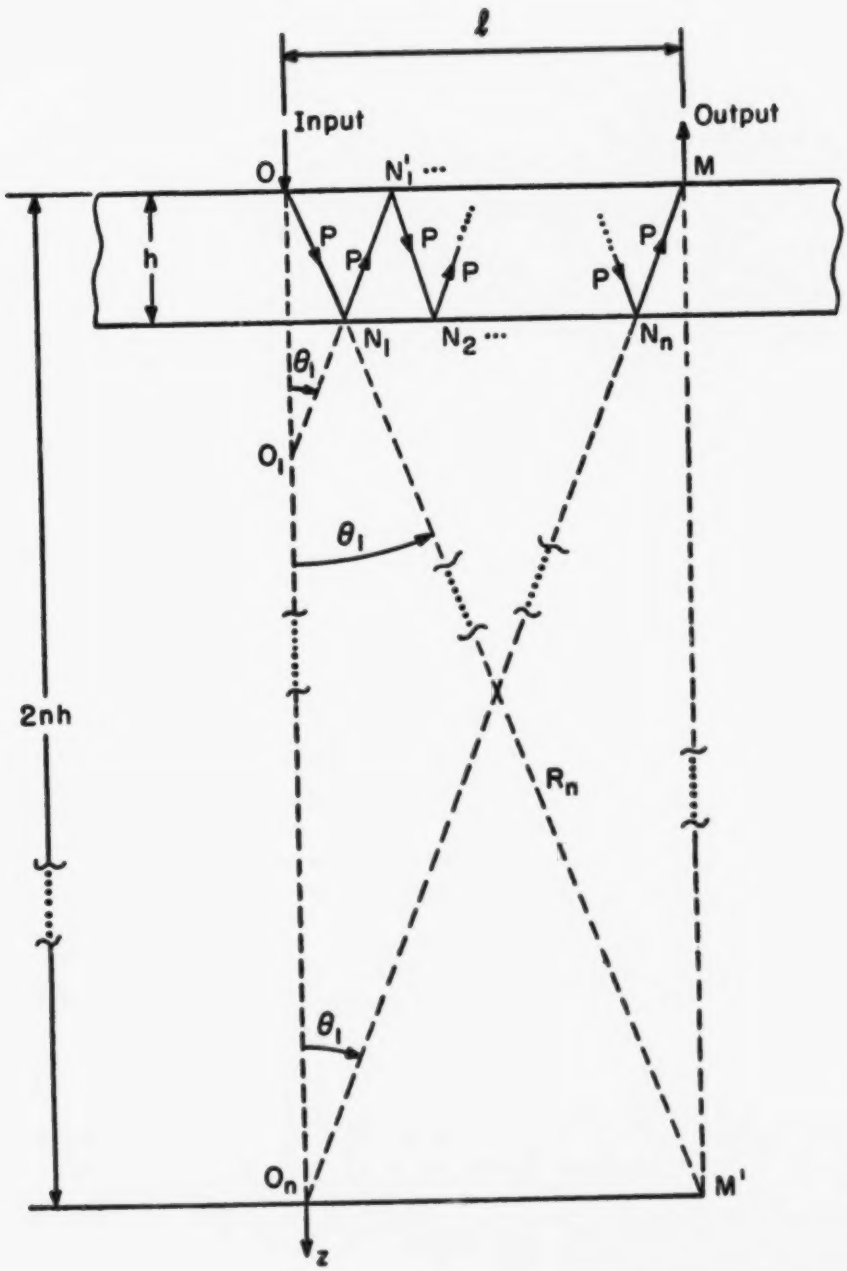

Fig. 4 The path of the P-P-... wave which arrives at the receiving transducer after n reflections from the bottom boundary.

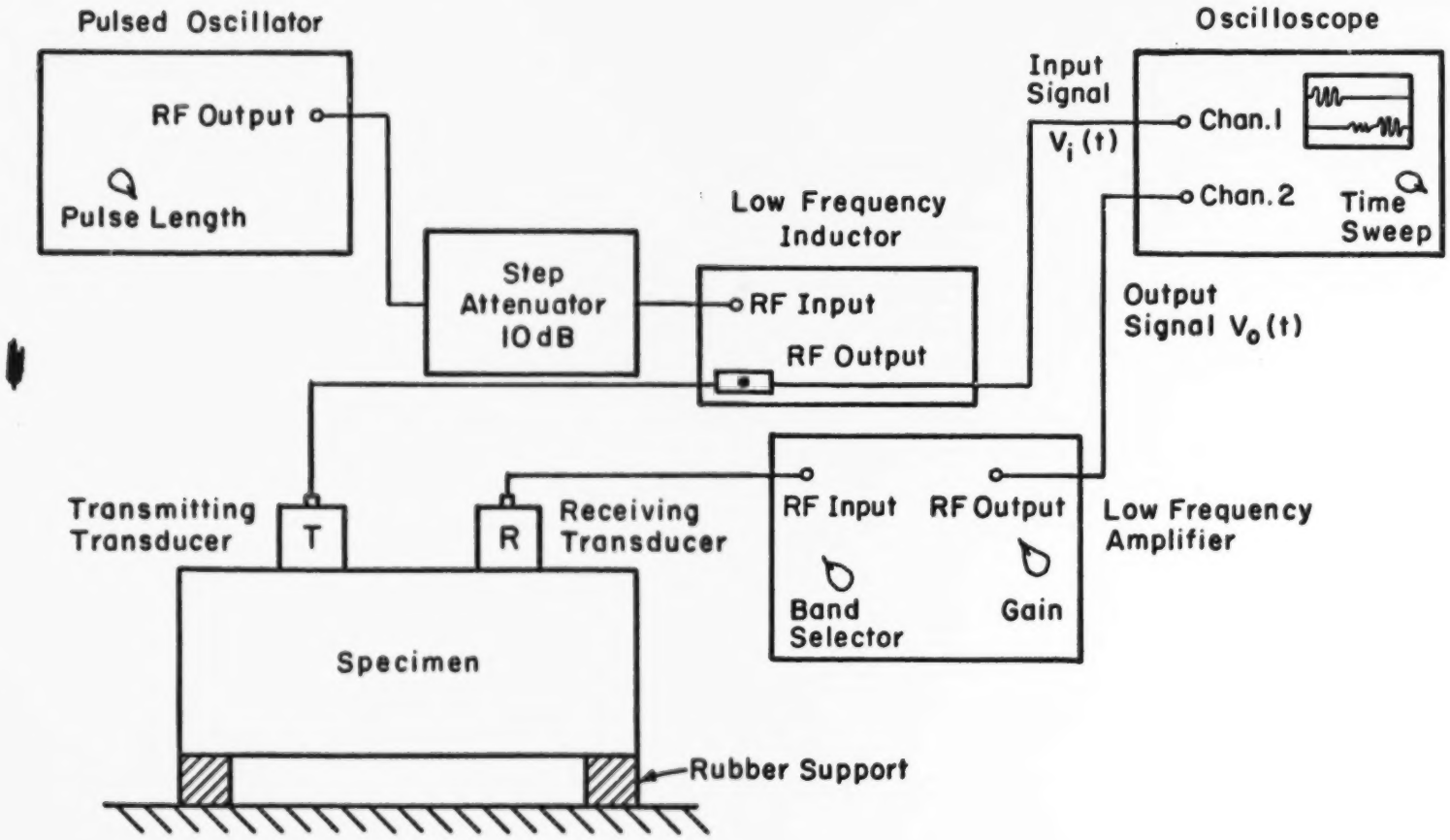

Fig. 5 Schematic of experimental system for measuring input-output for transmitting and receiving transducers coupled to the same face of a plate specimen.

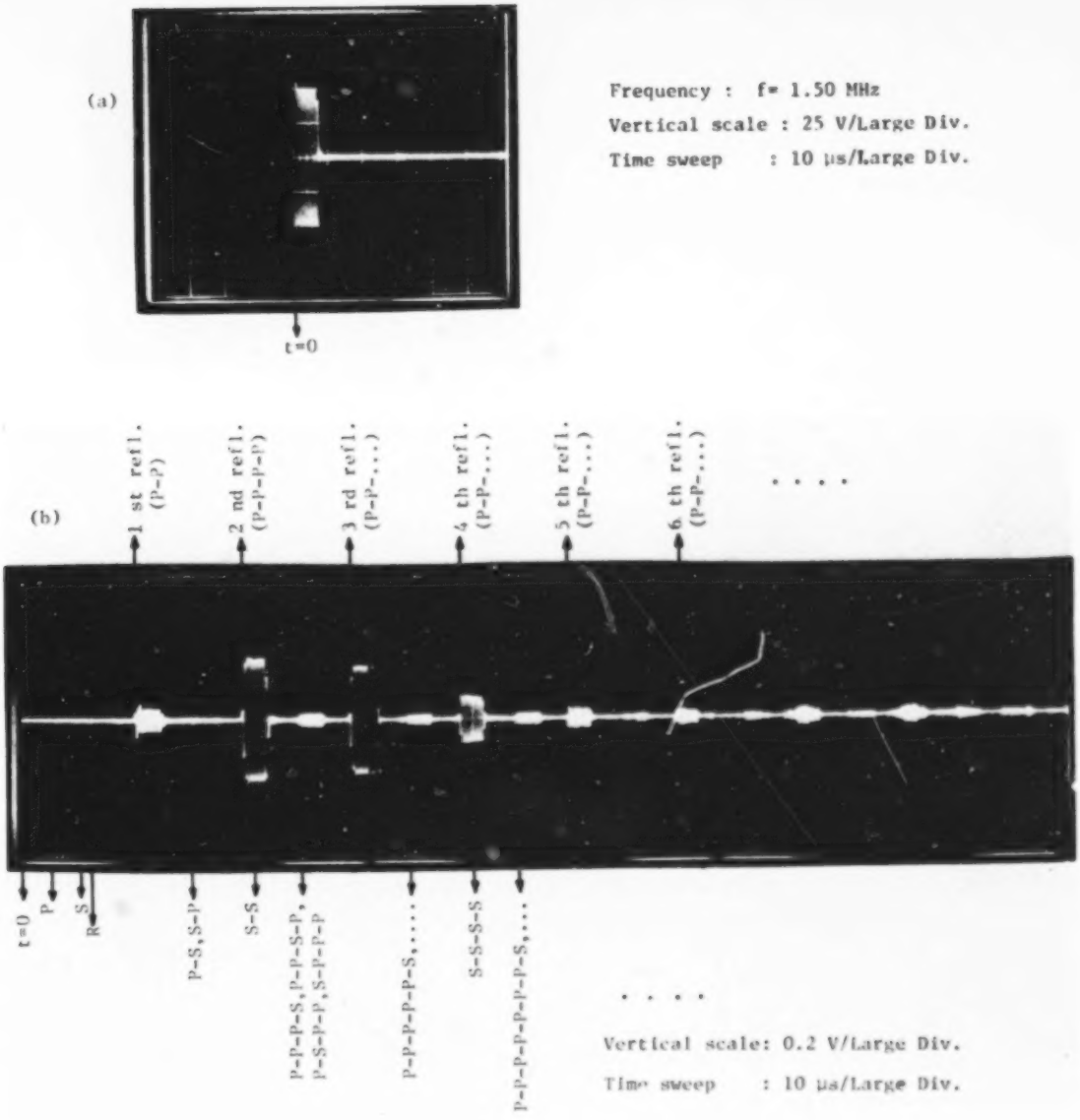

Fig. 6 Input signal (a) to the transmitting transducer and the corresponding output signal (b) from the receiving transducer at 1.50 MHz and a separation between transducers of 5.5 cm.

BEST DOCUMENT AVAILABLE

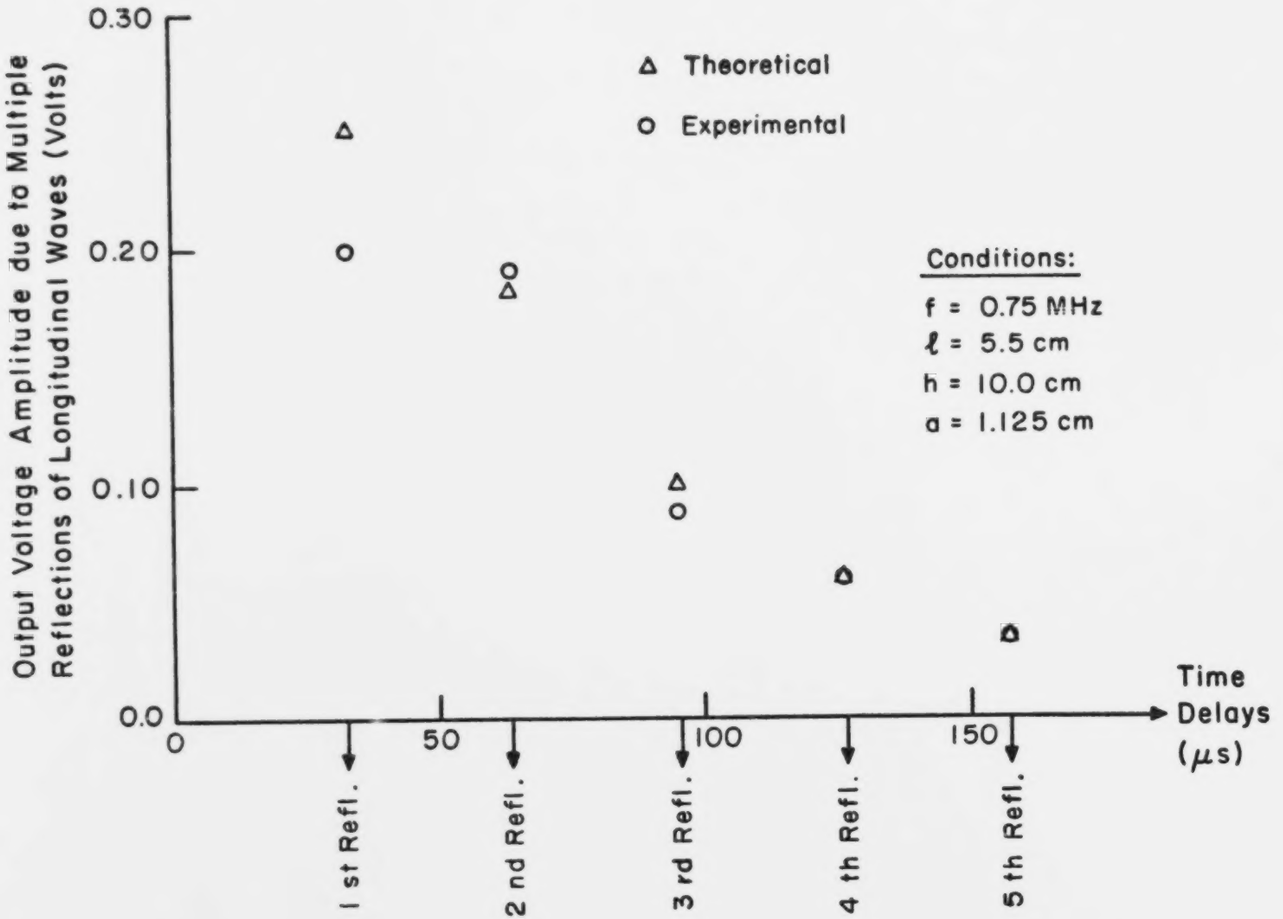

Fig. 7 Theoretical and experimental results for the output voltage amplitudes due to multiple reflections of longitudinal waves from the bottom face at 0.75 MHz and a separation between transducers of 5.5 cm.

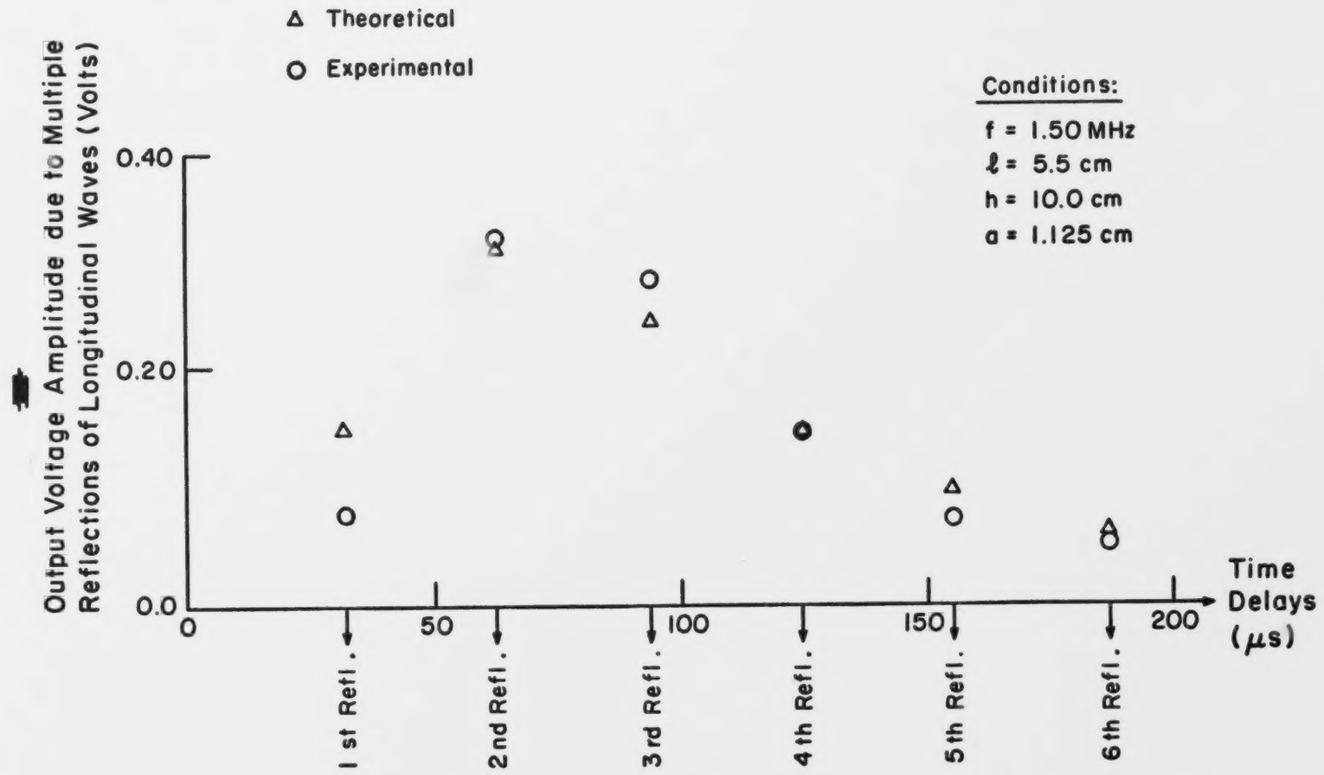

Fig. 8 Theoretical and experimental results for the output voltage amplitudes due to multiple reflections of longitudinal waves from the bottom face at 1.50 MHz and a separation between transducers of 5.5 cm.

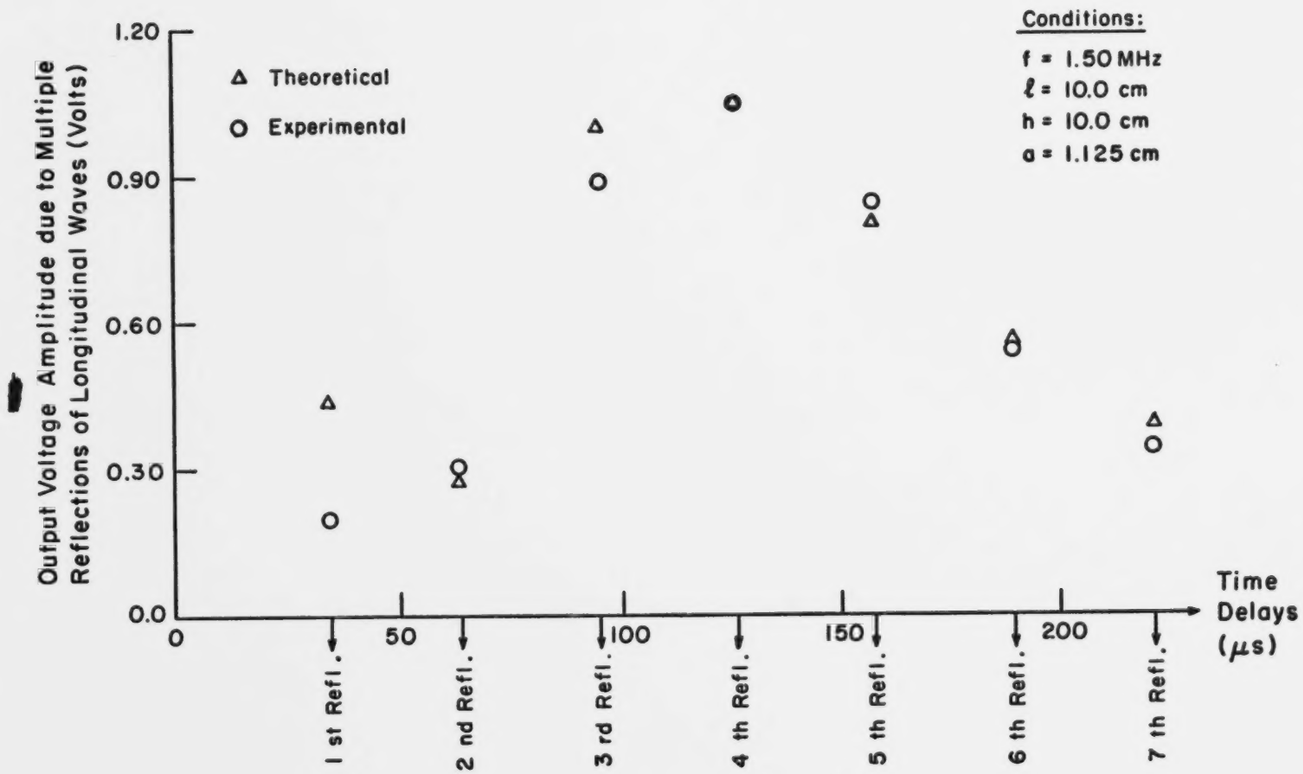

Fig. 9 Theoretical and experimental results for the output voltage amplitudes due to multiple reflections of longitudinal waves from the bottom face at 1.50 MHz and a separation between transducers of 10.0 cm.

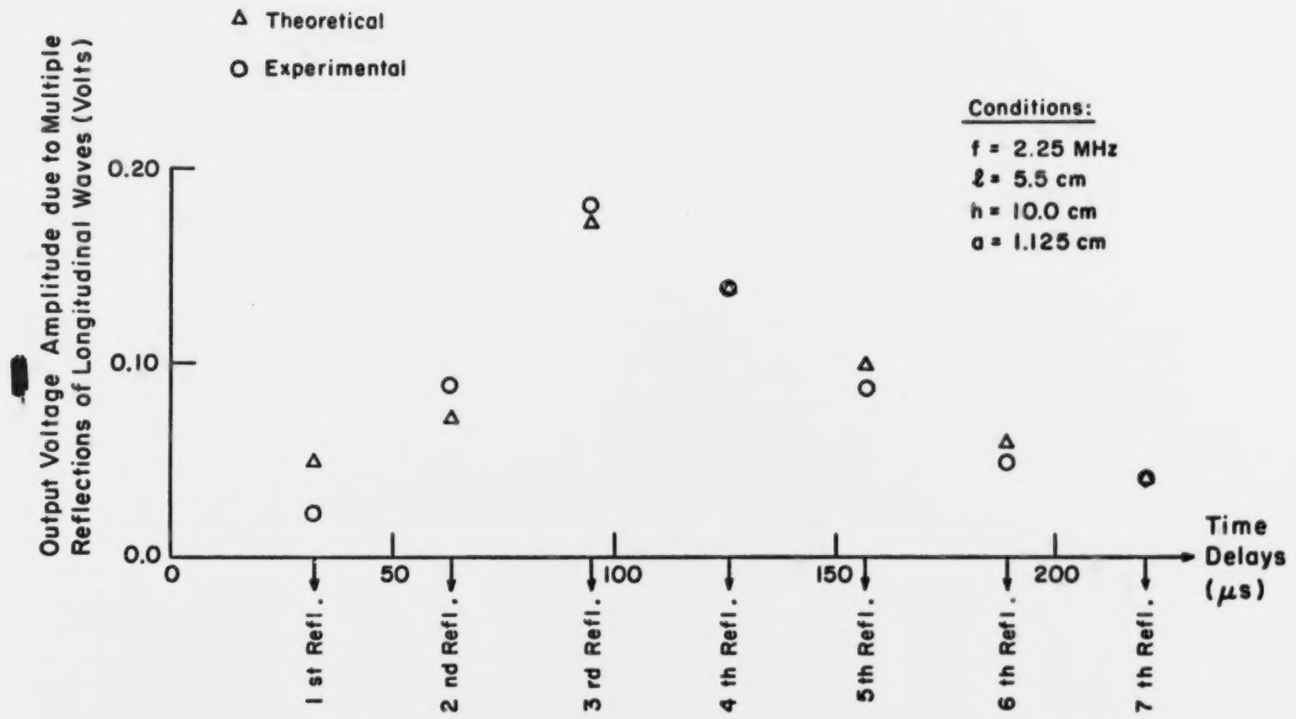

Fig. 10 Theoretical and experimental results for the output voltage amplitudes due to multiple reflections of longitudinal waves from the bottom face at 2.25 MHz and a separation between transducers of 5.5 cm.

E-1012

1. Report No. NASA CR-3506	2. Government Accession No.	3. Recipient's Catalog No.
4. Title and Subtitle ULTRASONIC INPUT-OUTPUT FOR TRANSMITTING AND RECEIVING LONGITUDINAL TRANSDUCERS COUPLED TO SAME FACE OF ISOTROPIC ELASTIC PLATE		5. Report Date February 1982 6. Performing Organization Code
7. Author(s) James H. Williams, Jr., Hira Karagulle, and Samson S. Lee		8. Performing Organization Report No. None 10. Work Unit No.
9. Performing Organization Name and Address Massachusetts Institute of Technology Department of Mechanical Engineering Cambridge, Massachusetts 02139		11. Contract or Grant No. NSG-3210 13. Type of Report and Period Covered Contractor Report
12. Sponsoring Agency Name and Address National Aeronautics and Space Administration Washington, D.C. 20546		14. Sponsoring Agency Code 505-33-22

15. Supplementary Notes

Final report. Project Manager, Alex Vary, Materials Division, NASA Lewis Research Center, Cleveland, Ohio 44135.

16. Abstract

Ultrasonic input-output characteristics for an isotropic elastic plate with transmitting and receiving longitudinal transducers coupled to the same face are analyzed theoretically and experimentally. In the theoretical analysis, it is assured that the transmitting ultrasonic transducer transforms electrical voltage into a uniform normal stress and vice versa for the receiving transducer. The asymptotic normal stress is calculated for an isotropic elastic half space subjected to a uniform harmonic normal stress applied to a circular region at the surface. Then the radiated stress waves are traced within the plate by considering wave reflections at the top and bottom faces. The output voltage amplitude of the receiving transducer is estimated by considering only longitudinal waves. Experiments are conducted on a 10 cm thick aluminum plate at 0.75, 1.50 and 2.25 MHz with separation distances between the transmitting and receiving transducers of 5.5 and 10.0 cm. There is a good agreement between the theoretical and experimental results for the output voltage wave packet amplitudes and times of arrival due to multiple reflections of the longitudinal waves. This study provides a major step towards the quantitative understanding of ultrasonic nondestructive evaluation parameters such as the stress wave factor.

17. Key Words (Suggested by Author(s))	18. Distribution Statement
Ultrasonic; Ultrasonic waves; Elastic waves; Isotropic media; Elastic media; Stress waves; Waveform analysis; Attenuation; Elastic moduli	Unclassified - unlimited STAR Category 38

19. Security Classif. (of this report)	20. Security Classif. (of this page)	21. No. of Pages	22. Price*
Unclassified	Unclassified	28	A03

* For sale by the National Technical Information Service, Springfield, Virginia 22161

NASA-Langley, 1982